Research Paper

PAIN®

OPEN VIDEO

miR-1306-3p directly activates P2X3 receptors in primary sensory neurons to induce visceral pain in rats

Yan-Yan Wu[a,b], Qian Wang[c], Ping-An Zhang[a], Cheng Zhu[d], Guang-Yin Xu[a,*]

Abstract

Mounting evidence indicates that microRNAs (miRNAs) play critical roles in various pathophysiological conditions and diseases, but the physiological roles of extracellular miRNAs on the disease-related ion channels remain largely unknown. Here, we showed that miR-1306-3p evoked action potentials and induced inward currents of the acutely isolated rat dorsal root ganglion (DRG) neurons. The miR-1306-3p–induced effects were significantly inhibited by A317491, a potent inhibitor of the P2X3 receptor (P2X3R), or disappeared after the knockdown of P2X3Rs in DRG neurons. We further identified R180, K315, and R52 as the miR-1306-3p interaction sites on the extracellular domain of P2X3Rs, which were distinct from the orthosteric ATP-binding sites. Intrathecal injection of miR-1306-3p produced visceral pain but not somatic pain in normal control rats. Conversely, intrathecal application of a miR-1306-3p antagomir and A317491 significantly alleviated visceral pain in a rat model of chronic visceral pain. Together, our findings suggest that miR-1306-3p might function as an endogenous ligand to activate P2X3Rs, eventually leading to chronic visceral pain.

Keywords: MiR-1306-3p, P2X3R, Dorsal root ganglion, Chronic visceral pain

1. Introduction

Chronic visceral pain is one of the most common chronic pain conditions and affects up to 25% of the population worldwide, substantially reducing the quality of life and work productivity in the patients.[9] Merging evidence suggested that peripheral sensitization is a fundamental mechanism underlying chronic visceral pain.[28] Sensitization of peripheral afferent nerves includes the increases in excitability of primary sensory neurons, neural transmitter release, and synaptic transmission at the spinal cord level.[30] The elevated activities of ion channels are a key regulator in peripheral sensitization.[3,51,65] Many channels/receptors, including the ionotropic channels and metabotropic receptors, are implicated in the generation and transmission of pain signals.[14,31] Among those, the purinergic P2X receptor channels play key roles in chronic visceral pain.[53,57] Seven mammalian P2X receptor subtypes, denoted as P2X1–P2X7, mainly expressed in the dorsal root ganglion (DRG) neurons.[8,27] Notably, the expression level of P2X3Rs in DRG neurons is significantly higher than that of other receptor subtypes.[7,10,25,43] As the orthosteric ligand of P2X3Rs, adenosine triphosphate (ATP) is a well-known extracellular signal molecule and widely present in the peripheral nervous system or the surrounding tissues.[2] Extracellular ATP triggers downstream signaling by activating 2 types of P2 purinergic receptors (P2X and P2Y) on cell membranes, leading to peripheral sensitization.[6,35] However, blocking P2X receptor function by inhibiting its ATP-binding sites did not completely relief pain sensitization. Therefore, it is vital to explore alternative mechanisms under pathophysiological conditions.

As a novel mechanism of regulating neuron functions and sensation, the release of extracellular vesicles containing microRNAs (miRNAs) often accompanied with the secretion of neurotransmitters.[26] In addition to the role of affecting channel protein expressions,[48] a recent study showed that miR-711 binds to the extracellular fragment of transient receptor potential A1 (TRPA1) receptors on DRG neurons, activates the TRPA1 channels, and alters a downstream signaling pathway and eventually the peripheral neurogenesis of itching.[15] In chronic pains, miRNAs may also play important roles, as recent studies demonstrated a large number of extracellular miRNAs related to expression and function of P2X3Rs.[38,50,63] However, it is unclear whether any miRNAs directly activate the extracellular fragment of P2X3Rs.

Sponsorships or competing interests that may be relevant to content are disclosed at the end of this article.

Y.-Y. Wu, Q. Wang, and P.-A. Zhang contributed equally to this work.

[a] Jiangsu Key Laboratory of Neuropsychiatric Diseases and Institute of Neuroscience, Soochow University, Suzhou, Jiangsu, P.R. China, [b] School of Life Sciences and Research Center for Resource Peptide Drugs, Shaanxi Engineering and Technological Research Center for Conversation and Utilization of Regional Biological Resources, Yanan University, Yanan, P. R. China, [c] Department of Anesthesiology, Children's Hospital of Soochow University, Suzhou, P.R. China, [d] Tianjin Key Laboratory of Function and Application of Biological Macromolecular Structures, School of Life Sciences, Tianjin University, Tianjin, P.R. China

**Corresponding author. Address: Laboratory of Translational Pain Medicine, Institute of Neuroscience, Soochow University, Suzhou 215123, P.R. China. Tel.: +86-512-65882817; fax: +86-512-65883602. E-mail address: guangyinxu@suda.edu.cn (G.-Y. Xu).*

Supplemental digital content is available for this article. Direct URL citations appear in the printed text and are provided in the HTML and PDF versions of this article on the journal's Web site (www.painjournalonline.com).

PAIN 164 (2023) 1555–1565

http://dx.doi.org/10.1097/j.pain.0000000000002853

In a preliminary study, we showed that the expression of miR-1306-3p elevated in DRG neurons using a rat model of chronic visceral pain. Furthermore, we have demonstrated that P2X3Rs are crucial for chronic visceral pain.[52,53,60] Hence, in this study, we hypothesize that the upregulated miR-1306-3p contributed to chronic visceral pain by directly interacting with the purinergic P2X3Rs in DRG neurons. Using an array of techniques including patch-clamp recordings, gene silencing, and computational simulations, we verified that miR-1306-3p quickly evoked action potentials and induced inward currents of rat DRG neurons. Further experiments unveil the key interaction sites of miR-1306-3p on the P2X3R extracellular domain. More importantly, our study suggests that a combined application of ATP antagonist and miRNA–antagomir can be a novel and powerful strategy for the treatment of chronic visceral pain in patients.

2. Materials and methods

2.1. Animals and induction of chronic visceral pain

Sprague-Dawley (SD) male rats weighing 200 to 250 g were selected for this study, which were approved by the Ethics Committee of Soochow University and purchased by Soochow University Laboratory Animal Center (license number: SYXK 2007-0035). To avoid the periodic effects of estrogen on pain, we did the studies only on male rats for ensuring the uniformity and repeatability of experiments.[23,32,61] The room temperature was controlled at 22 ± 2°C, and the light cycle was automatically controlled (light/dark 12-hour cycle). Chronic visceral pain was induced by neonatal colonic inflammation (NCI) as described previously.[56] Briefly, 0.5% acetic acid was injected anally into male rats on their 10th day of life, and the experiment was performed at 6 weeks of age.

2.2. MicroRNA chip

MicroRNA microarray was used to detect the differential distribution and expression of DRG-derived exosomal miRNAs in NCI rats and normal controls. This part of the experiment was tested by company Suzhou Yingze Biomedical Technology Co, Ltd (Suzhou, China).

2.3. Constructs and drug application

The cDNA plasmids of rat pEX-4-*rP2X3R*, pEX-4-$rP2X3R^{K63A+K65A+F174A+R281A}$, pEX-4-$rP2X3R^{R180A}$, pEX-4-$rP2X3R^{K242A}$, pEX-4-$rP2X3R^{W253A}$, pEX-4-$rP2X3R^{K315A}$, pEX-4-$rP2X3R^{R52A}$, pEX-4-$rP2X3R^{K251A}$, pEX-4-$rP2X3R^{K259A}$, pEX-4-$rP2X3R^{R52A+R180A+K315A}$, miR-1306-3p antagomir, and a negative control (NC) of miR-1306-3p antagomir were all purchased from GenePharma (Shanghai, China). For the animal behavior tests, single intrathecal injection of different concentrations of miR-1306-3p, miR-1306-3p antagomir, and miR-1306-3p antagomir NC (5, 20, and 100 μM/10 μL) was injected into the subarachnoid space between the lumbar vertebrae (L4-L5) of rats with the age of 6 weeks. After injection, the needle was stayed for 10 seconds to prevent the drug leak.[50]

2.4. Pain behavioral tests

All behaviors were tested in a blind manner. Rats were first habituated to the environment for at least 3 days before the testing.

2.4.1. For visceral pain

Colorectal distension (CRD) was used to induce chronic visceral pain behaviors as described previously.[19] Briefly, under mild sedation (inhalation anesthesia by isoflurane), a flexible latex balloon (5 cm) attached to Tygon tubing was inserted 7 cm into the rectum and descending colon through the anus and held in place by taping the Tygon tubing to the tail. Rats were placed in small lucite cubicles and allowed to adapt for 30 minutes. To minimize possible insult from the repetitive distension of the colon, the CRD threshold was measured as the minimal distension pressure in millimeters of mercury to evoke an abdominal visceromotor response to a steady increase in distension pressure through a sphygmomanometer.

2.4.2. For mechanical sensitivity

Experiments were performed on rats before and after miR-1306-3p injection (20 μM/10 μL). The hind paw withdrawal threshold (PWT) in response to stimulation of von Frey filaments was measured as described previously.[34,64] The tactile stimulus producing a 50% likelihood of withdrawal was determined using the "up-down" calculating method. We determined the 50% paw withdrawal threshold by Dixon's up-down method.[5,12]

2.4.3. For thermal sensitivity

Thermal sensitivity was tested using Hargreaves radiant heat apparatus.[16,64] To avoid injury to the plantar of rats, the automatic cutoff time was 25 seconds. The average thermal paw withdrawal latencies (PWL) value was calculated.

2.4.4. Rotarod test

To observe the drug effect on rat motor function, the rotarod test was used as described previously.[36,39]

2.5. Dissociation of dorsal root ganglion neurons

Isolation of DRG neurons from adult male SD rats was performed as reported previously.[4,45] The dissection solution contained the following (in mM): 130 NaCl, 5 KCl, 2 KH_2PO_4, 1.5 $CaCl_2$, 6 $MgSO_4$, 10 glucose, and 10 HEPES, adjusted to pH 7.2 with NaOH and osmolarity 305 mOsm. Dorsal root ganglion cells were plated on glass coverslips at room temperature for 1 hour before whole-cell patch-clamp recordings.

2.6. HEK293T cell cultures and transfections

HEK293T stable cell line (ATTC Cat# CRL-3216, RRID: CVCL_0063) was cultured in Dulbecco's modified eagle medium (DMEM) (Gibco, Shanghai, China), supplemented with 1% streptomycin, penicillin, and 10% fetal bovine serum, and maintained with 5% CO_2 in 37°C incubators. Transfection of rP2X3R or rTRPV1 (1 μg cDNA) was performed with Lipofectamine 2000 Reagent (Invitrogen, Shanghai, China) and cultured for 24 hours before electrophysiological and biochemical studies.[15,33]

2.7. Whole-cell patch-clamp recordings

Whole-cell patch-clamp recordings were performed at room temperature (~24°C) using a HEKA EPC-10. To test the effects of miRNAs on excitability of rat DRG neurons, resting membrane potential and action potential were recorded as described

previously.[58] The voltage was clamped at −60 mV. For DRG neurons' patch-clamp recording, the extracellular solution contained the following (in millimoles): 130 NaCl, 5 KCl, 2 KH_2PO_4, 2.5 $CaCl_2$, 1 $MgCl_2$, 10 HEPES, and 10 glucose, adjusted to pH 7.2 with NaOH and osmolarity 295 to 300 mOsm. The pipette solution contained the following (in millimoles): 140 potassium gluconate, 10 NaCl, 10 HEPES, 10 glucose, 5 BAPTA, and 1 $CaCl_2$, adjusted to pH 7.25 with KOH and osmolarity 295 mOsm. To test the effects of miRNAs on HEK293-transfected cells, the recording pipette resistance was 6 to 8 MΩ. The pipette solution contained the following (in mM): 147 NaCl, 2 KCl, 10 HEPES, and 10 EGTA, adjusted to pH 7.3 with NaOH and osmolarity 295 to 315 mOsm. The extracellular solution contained the following (in mM): 147 NaCl, 10 HEPES, 13 D-glucose, 2 KCl, 2 $CaCl_2$, and 1 $MgCl_2$, adjusted to pH 7.3 with NaOH and osmolarity 295 to 315 mOsm.[20] The current density, activation time (10%-90% of the channel opening time), and inactivation time constant were determined. The current traces were measured at different holding potentials (−100 mV ~ +40 mV, step 20 mV) for current–voltage curves.

2.8. Calcium imaging

Calcium imaging was conducted to test the effect of miRNA on rat T13-L2 DRG neurons as described previously.[47]

2.9. Measurement of membrane protein

After transfection, the HEK293T cells were washed with phosphate buffer solution (PBS) and centrifuged at a speed of 300*g* for 5 minutes to collect cell precipitation. P2X3R membrane protein expression was extracted by using Mem-PER Plus Membrane Protein Extraction Kit (Thermo Scientific, Shanghai, China) according to the manufacturer's instruction.[58] Polyvinylidene fluoride was incubated with anti-P2X3R (Alomone Labs Cat# APR-026, RRID: AB_2341052, Shanghai, China) and anti-Na+-K+-ATPase (Abcam Cat# 2047-1, RRID: AB_991679, Shanghai, China) overnight at 4°C. Anti-rabbit HRP-conjugated (MultiSciences Cat# GAR007, RRID: AB_2827833, Hangzhou, China) antibodies were incubated for 2 hours at room temperature. Immunoreactive proteins were detected by enhanced chemiluminescence (ECL kit; GE HealthcarePharmacia Biotech, Shanghai, China). Band intensities were measured using ImageJ software (Bio-Rad, Hercules, CA). ND7-23 cell line (ECACC Cat# 92090903, RRID: CVCL_4259) was used to detect potent interfering RNA of P2X3Rs.[33]

2.10. Molecular modeling

The secondary and tertiary structures of miR-1306-3p were modeled by CentroidFold[37] and 3dRNA,[46] respectively. The complex model of miR-1306-3p and P2X3Rs was generated by HDOCK[54] with default parameters using the crystal structures of P2X3 (PDB 5SVJ: apo or closed state; PDB 5SVK: open state) as inputs.

The 100 ns all-atom simulations of the complexes of P2X3 and miRNA were performed with the Gromacs 2019.6 package and the CHARMM36 force field.[18,41] The membrane components (POPC[1-palmitoyl-2-oleoyl-sn-glycero-3-phosphocholine], POPE[1-palmitoyl-2-oleoyl-sn-glycero-3-phosphoethanolamine], POPS[1-palmitoyl-2-oleoyl-sn-glycero-3-hosphatidylserine], and cholestanol) were built by CHARMM-GUI.[49] The system was then solvated with TIP3P waters, neutralized with 150 mM KCl, minimized using the steepest descent method to relieve unfavorable contacts, and then equilibrated with 6 cycles of reducing force constants before the production run. The simulations were performed at 300 K (velocity-rescale thermostat) and constant pressure (1 bar, Parrinello–Rahman constant-pressure and constant-temperature ensemble). A 10 Å cutoff was set for nonbonded interactions, and the particle mesh Ewald method was used for electrostatics calculations. LINear Constraint Solver (LINCS) were applied to H-bonds, and the time step was 2 fs. After reaching the equilibrium, representative binding conformations were extracted and analyzed based on root-mean-square deviation (RMSD) calculations. The key interaction sites on P2X3Rs were further verified by constructing plasmid vectors with different mutations.

2.11. Data analysis

All data were expressed as mean ± SEM. GraphPad_Prism_8.3 was applied to statistical analyses. Statistical significance for parametric data was analyzed by the Student *t* test for comparison between 2 groups and by analysis of variance followed by the Tukey test for multiple comparisons. A *P* value of less than 0.05 was considered statistically significant.

3. Results

3.1. MiR-1306-3p evoked chronic visceral pain

We first characterized the contents of miRNAs in the exomes derived from T13-L2 DRG neurons using miRNA chip assays, which varied significantly in NCI rats compared with the control rats (CON) (**Fig. 1A**). Specifically, the expression of miR-1306-3p featured 37% elevation in DRG tissue of NCI rats (**Fig. 1B**), and it was not altered in the spinal cord nor the brain tissues (Fig. S1A-B, available as supplemental digital content at http://links.lww.com/PAIN/B768). Indeed, the intrathecal injection of miR-1306-3p significantly produced visceral pain on control healthy rats (**Fig. 1C**), whereas the intrathecal injection of miR-1306-3p antagomir markedly reduced visceral pain of NCI rats (**Fig. 1D**), but it has no effect on somatic pain (Fig. S1C-G, available as supplemental digital content at http://links.lww.com/PAIN/B768). We further examined the function of miR-1306-3p using whole-cell current clamp. The miR-1306-3p (20 μM) puff directly induced action potentials of the dissociated DRG neurons in vitro (**Fig. 1E**), whereas other miRNAs did not (Fig. S1H-N, available as supplemental digital content at http://links.lww.com/PAIN/B768). The application of miR-1306-3p (20 μM) in vitro also increased the calcium responses of DRG neurons (**Fig. 1F**). We then explored the mechanism by which miR-1306-3p evoked action potentials. Under the whole-cell voltage-clamp mode, the miR-1306-3p puff rapidly induced voltage-dependent inward current, probably mediated by nonselective cation channels (**Fig. 1G**). The currents induced by miR-1306-3p in DRG neurons increased in a dose-responsive manner and were quantified by the plot of current density and miR-1306-3p concentrations (**Fig. 1H**), suggesting a specific interaction between miR-1306-3p and DRG cellular components (eg, P2XRs). Furthermore, the current induced by miR-1306-3p showed a tendency to desensitize after repeated applications (Fig. S1O, available as supplemental digital content at http://links.lww.com/PAIN/B768). Together, our data suggested that miR-1306-3p participated in chronic visceral pain, and its effects were mediated by the activation of DRG neurons.

3.2. MiR-1306-3p directly activates P2X3Rs

We next analyzed the mechanism by which miR-1306-3p induced inward currents on DRG neurons and focused on the highly expressed P2X3R. The extracellular surface of the P2X3R contains

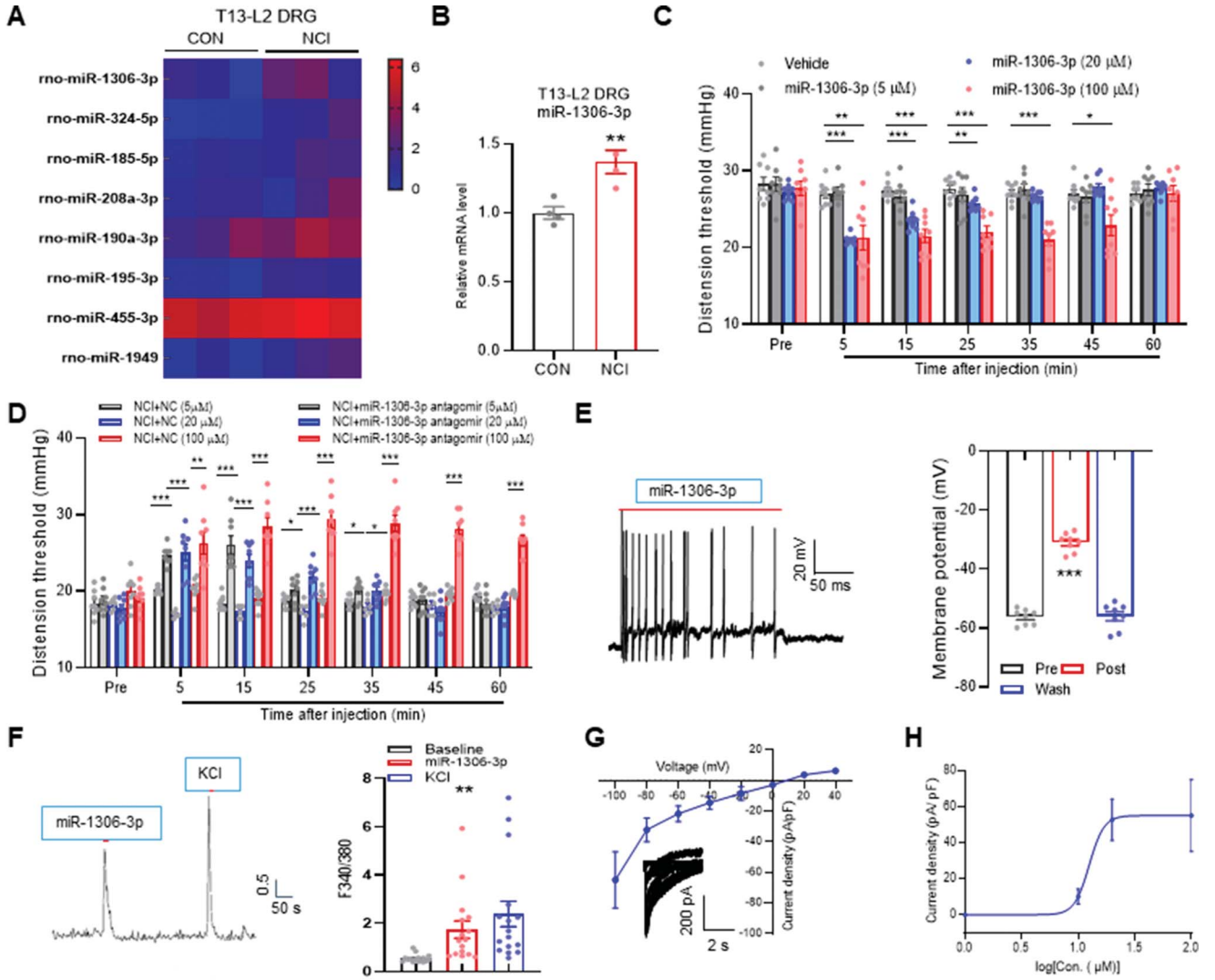

Figure 1. MiR-1306-3p in rat DRG neurons mediated chronic visceral pain. (A) Heat map of DRG exosome miRNA microarray of NCI and CON rats (n = 3 rats for each group). (B) Quantification of real-time PCR (qPCR) assays showing a significant upregulation of miR-1306-3p mRNA expression in T13–L2 DRG neurons of NCI rats compared with age-matched CON rats (n = 4 rats for each group, $^{**}P < 0.01$, *t* test). (C) The dose–response and time course of CRD thresholds in NCI rats given miR-1306-3p antagomir or the same volume of antagomir-NC (n = 8 rats for each group, $^{***}P < 0.001$, $^{**}P < 0.01$, and $^{*}P < 0.05$, one-way ANOVA). (D) The dose–response and time course of CRD thresholds in CON rats given miR-1306-3p were significantly lower than those in age-matched CON rats (n = 8 rats for each group, $^{***}P < 0.001$, $^{**}P < 0.01$, and $^{*}P < 0.05$, vs vehicle, one-way ANOVA). (E) Traces and the bar graph statistics of miR-1306-3p induced action potentials in DRG neurons of normal rats (n = 8 cells, $^{***}P < 0.001$, vs vehicle, one-way ANOVA). (F) Traces and bar graph statistics of miR-1306-3p induced calcium responses in DRG neurons of normal rats compared with baseline (n = 13 cells, $^{**}P < 0.01$, vs baseline group). (G) Voltage dependence of miR-1306-3p induced inward currents. Examples of current–voltage (I–V) relationships of peak induced by miR-1306-3p. The current traces were measured at different holding potentials. The current traces were shown as the inset of each I–V curve (n = 8 cells). (H) Dose–response curve of miR-1306-3p–evoked currents. The peak currents were plotted as a function of miR-1306-3p concentration. The dose–response curve was fit by the Hill equation (EC50 = 12.51 μM; Hill slope = 6.649; 1 μM, n = 8; 10 μM, n = 8; 20 μM, n = 18; and 100 μM, n = 15). ANOVA, analysis of variance; CRD, colorectal distension; DRG, dorsal root ganglion; miRNA, microRNA; NC, negative control.

continuous regions enriched with positive charges (blue area, **Fig. 2A**),[29] which may attract the negatively charged phosphodiester backbones of miRNAs. Incubation of A317491, an antagonist of P2X3Rs, significantly reduced the miR-1306-3p–induced inward currents, action potentials, and calcium responses in DRG neurons (**Figs. 2B–D**). We further designed 3 siRNAs to silence the P2X3Rs transfected in ND7-23 cell line (DRG cell line, **Fig. 2E**). Intrathecal injection of siP2X3R-3 for 1 week significantly reduced inward current stimulated by miR-1306-3p (**Fig. 2F**). Hence, miR-1306-3p may directly activate P2X3Rs. Indeed, the intrathecal injection of A317491 blocked the miR-1306-3p–induced effects and reversed the visceral hyperalgesia caused by miR-1306-3p in CON rats (**Fig. 2G**). Our results strongly suggested that the miR-1306-3p–induced current is mediated by the activation of P2X3Rs.

3.3. MiR-1306-3p activates dorsal root ganglion neurons not through other membrane receptor but its main sequence nucleotide combined with P2X3Rs

In addition, we examined 2 other membrane ion channels (TRPV1 and $Na_v1.7$) of DRG neurons by a combination of structural models and cellular experiments. Unlike P2X3Rs, the electrostatic surface of transient receptor potential vanilloid 1 (TRPV1) and $Na_v1.7$ indicated the location of charged regions mainly at the cytoplasmic side (**Figs. 3A–E**). For the TRPV1 expressing HEK293T cells, miR-1306-3p did not induce any inward current (**Fig. 3C**), nor did capsazepine (CPZ, 10 μM, a TRPV1-specific inhibitor) block the miR-1306-3p–induced currents on DRG neurons (**Fig. 3B**). Similarly, tetrodotoxin (TTX, 1 μM, a typical sodium channel inhibitor) did not block the

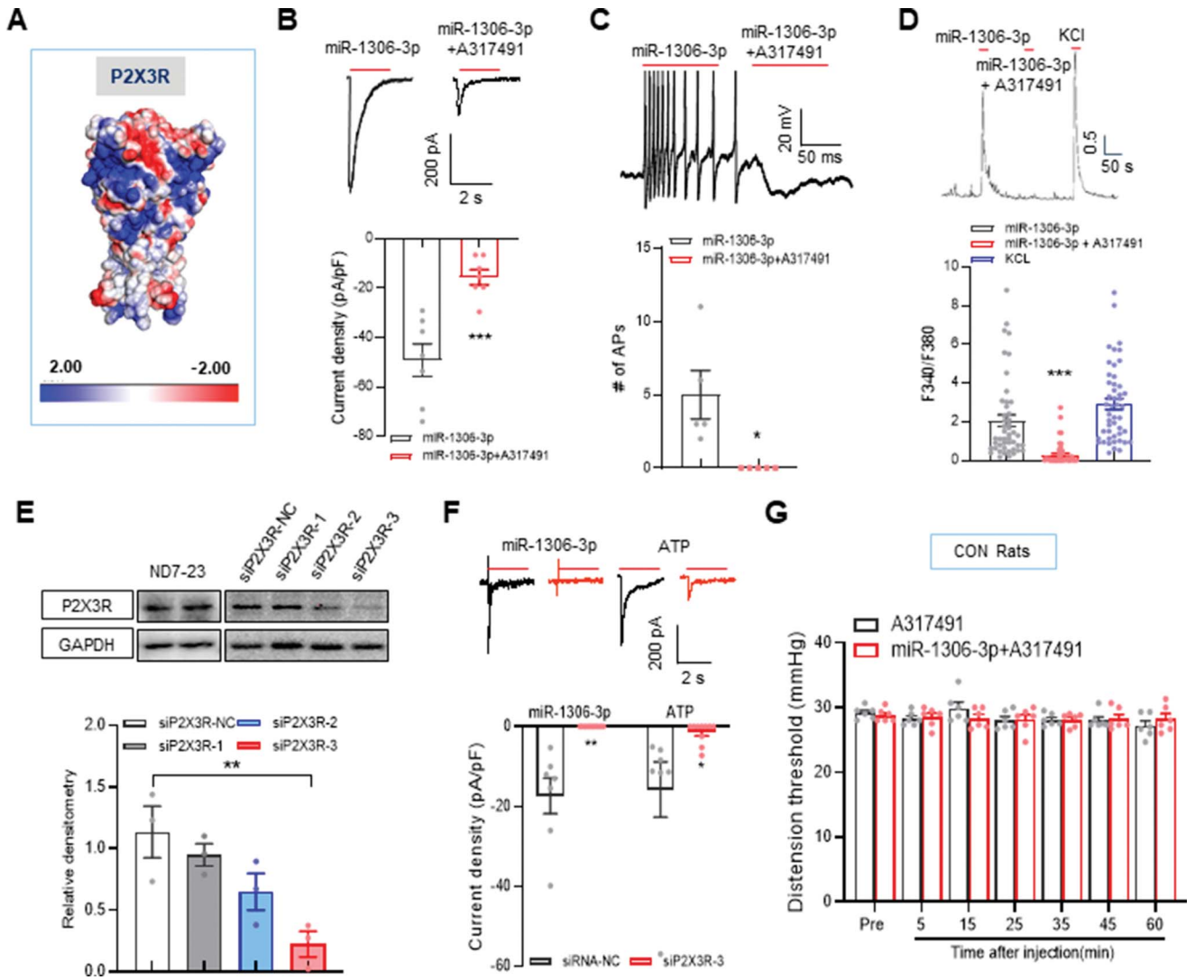

Figure 2. MiR-1306-3p activates DRG neurons through binding to P2X3Rs. (A) P2X3R was illustrated as the electrostatic potential surfaces. (B) P2X3R antagonist (A317491) significantly reduced the current induced by miR-1306-3p. Representative profiles of the currents induced by miR-1306-3p and the mix of miR-1306-3p and A317491 (10 μM, top right). Bottom, bar graph showing the reduction of the current density (n = 7 cells, $^{***}P < 0.001$, *t* test). (C) P2X3R antagonist A317491 significantly blocked action potentials induced by miR-1306-3p. Top, the patterns of action potential induced by miR-1306-3p (left) or the mix of miR-1306-3p and A317491 (10 μM) (right). Bottom, bar graph statistics of action potentials (n = 5 cells, $^{*}P < 0.05$, *t* test). (D) P2X3R antagonist A317491 significantly blocked the calcium responses induced by miR-1306-3p. Top, the peaks of calcium response induced by miR-1306-3p (left), the mix of miR-1306-3p and A317491 (middle), and KCl (right) (30 mM), respectively. Bottom, bar graph statistics of ΔF340/380 signals (n = 47 cells, $^{***}P < 0.001$, *t* test). (E) Top: the expression of P2X3R in ND7-23 cell line with or without transfection of various siP2X3Rs (right). Bottom: siP2X3R-3 significantly reduced the expression levels of P2X3Rs. (F) Representative profiles and bar graph of the currents induced by miR-1306-3p (left) and ATP (right) on DRG neurons after the P2X3R has interfered by intrathecal injection of siP2X3R-3 for 1 week. (G) Intrathecal injection of A317491 blocked the miR-1306-3p–induced effects. Intrathecal injection of A317491 did not alter the CRD thresholds in CON rats (n = 6 rats, $^{**}P < 0.01$, $^{*}P < 0.05$, one-way ANOVA). ANOVA, analysis of variance; CRD, colorectal distension; DRG, dorsal root ganglion; KCl, potassium chloride; GAPDH, glyceraldehyde-3-phosphate dehydrogenase; ATP, adenosine triphosphate.

miR-1306-3p–induced inward currents (**Figs. 3D and E**). Above all, the results further suggest that the miR-1306-3p binds directly to P2X3Rs.

We further mutated the miR-1306-3p sequence in 7 different sites, namely, m1-7 (**Fig. 3F**). The abilities of these mutant products to induce inward currents were tested by electrophysiological methods in HEK293T cells transfected with the P2X3R plasmid. Overall, the miR-1306-3p-m2 mediated significantly decreased current when compared with that of miR-1306-3p (**Fig. 3G**). Intrathecal injection of miR-1306-3p-m2 did not produce chronic visceral pain neither (**Fig. 3H**), which was in consistent with the patch-clamp results. Hence, GTT of the miR-1306-3p sequence was the main nucleic acid bases binding to P2X3Rs.

3.4. MiR-1306-3p allosterically regulates P2X3R functions

We then performed molecular dockings between P2X3R and miR-1306-3p models (Fig. S2A-B, available as supplemental digital content at http://links.lww.com/PAIN/B768). The top-ranking complex models indicated that 4 amino acid residues of P2X3R (**Fig. 4A**) were closely related to the miR-1306-3p binding; they are arginine 180 (R180), lysine 259 (K259), lysine 315 (K315), and arginine 52 (R52). Next, we designed accordingly 4 single point mutation plasmids of P2X3Rs (**Figs. 4B–E**, red balls) and delineated their functions at the electrophysiological level. The R180, K315, and R52 single mutations all featured significantly reduced inward currents on miR-1306-3p binding (**Fig. 4F**, Fig.S2C-G, available as supplemental digital content at http://links.lww.com/PAIN/B768). We also identified

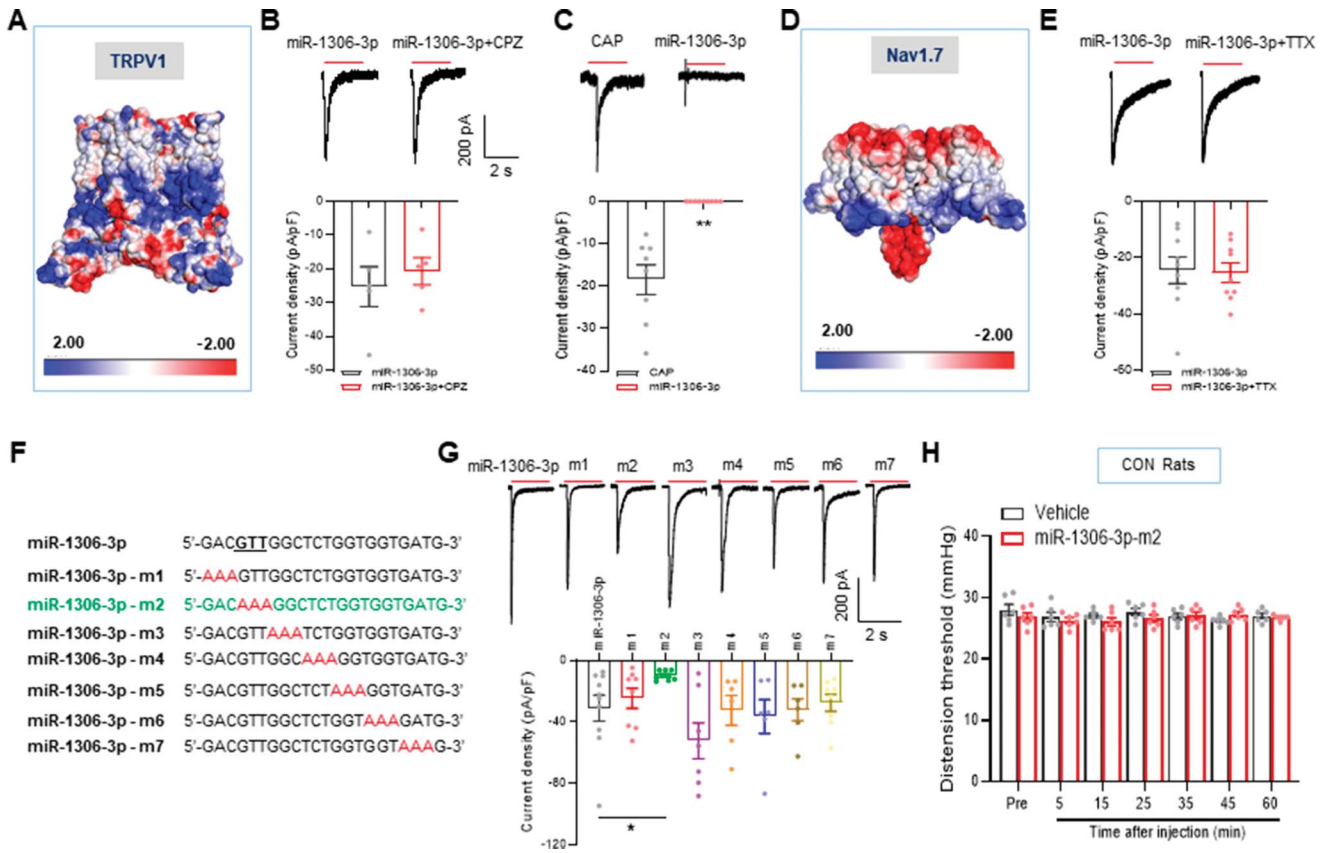

Figure 3. MiR-1306-3p activates DRG neurons not through other membrane receptor but its main sequence nucleotide combined with P2X3Rs.(A) TRPV1 was illustrated as the electrostatic potential surfaces. (B) TRPV1-specific blocking agent capsazepine had no impact on the current induced by miR-1306-3p on DRG neurons. Top: the trace of current induced by miR-1306-3p (left) and the mix of miR-1306-3p and CPZ (10 μM) (right). Bottom: bar graph (n = 6 cells, $P > 0.05$, *t* test). (C) Top: the example of current induced by capsaicin (CAP, 10 μM, left) and miR-1306-3p (right) on HEK293T cells that transfected with the plasmid of TRPV1. Bottom: histogram of capsaicin-induced current and miR-1306-3p–evoked current (n = 6 cells, $^{**}P < 0.01$, *t* test). (D) Sodium channel was illustrated as the electrostatic potential surfaces. (E) Sodium current antagonists (TTX, 1 μM) had no impact on the current induced by miR-1306-3p. Top: example of current induced by miR-1306-3p (left) and the mix of miR-1306-3p and TTX (right). Bottom: bar graph (n = 10 cells, $P > 0.05$, *t* test). (F) The nucleotide mutations were highlighted in red of the miR-1306-3p sequence variants. (G) Above, traces of the currents induced by miR-1306-3p and different mutants (m1-m7) in HEK293T cells that expressed the plasmid of P2X3Rs. Below, histogram of the current densities (miR-1306-3p, n = 12; m1, n = 9; m2, n = 7; m3, n = 7; m4, n = 7; m5, n = 6; m6, n = 7; and m7, n = 8. $^{*}P < 0.05$, one-way ANOVA). (H) Intrathecal injection of miR-1306-3p-m2 did not produce chronic visceral pain of healthy control rats (n = 6 for each group). ANOVA, analysis of variance; DRG, dorsal root ganglion; CPZ, capsazepine; TTX, tetrodotoxin.

4 key amino acids' ATP-binding site at P2X3Rs; they are lysine 63 (K63), lysine 65 (K65), phenylalanine 174 (F174), and arginine 281 (R281). We further obtained combined mutations of the miR-1306-3p and ATP-binding sites (rP2X3R$^{R180A+K315A+R52A}$ and rP2X3R$^{K63A+K65A+F174A+R281A}$, **Fig. 4G**, red balls and green balls, respectively). We observed ATP-induced currents in rP2X3R$^{R180A+K315A+R52A}$ expressing HEK293T cells, whereas the miR-1306-3p–induced currents were completely abolished (**Fig. 4H**, Fig. S2H, available as supplemental digital content at http://links.lww.com/PAIN/B768). On the other hand, miR-1306-3p induced inward currents in rP2X3R$^{K63A+K65A+F174A+R281A}$ expressing HEK293T cells, whereas the ATP-induced currents were suppressed (**Fig. 4I**, Fig. S2I, available as supplemental digital content at http://links.lww.com/PAIN/B768). The results suggested that R180, K315, and R52 played significant roles in miR-1306-3p binding and constituted an allosteric site for the regulation of P2X3R functions.

3.5. Molecular dynamics equilibrated conformations of the miR-1306-3p–P2X3R complex

To characterize the impact of miR-1306-3p binding on P2X3R structures and functions, we simulated the interactions between the miRNA and P2X3R at the apo state or ATP-bound, open state using all-atom molecular dynamics. At the apo state, miR-1306-3p enlarged the pore of the P2X3R channel from 7.5 Å to 11.8 Å (average values of apo or miR-1306-3p–bound conformations, respectively), which was slightly smaller than that of the open state (18.5 Å, **Figs. 5A and B**). We observed stable interactions between miR-1306-3p and P2X3R throughout the 100 ns simulations. Indeed, the activation time of miR-1306-3p (14.75 ± 2.87 ms) was significantly longer than that of ATP (6.63 ± 1.28 ms), indicating that miR-1306-3p stabilized the pore-opening conformations (**Fig. 5C**). Binding energy calculations based on simulated structures also indicated that miR-1306-3p likely facilitated the transition of P2X3R from apo to open states (Table S1, available as supplemental digital content at http://links.lww.com/PAIN/B768). Furthermore, there was no significant difference in inactivation time between miR-1306-3p (612.62 ± 250.44 ms) and ATP (641.13 ± 201.81ms, Fig. S3A, available as supplemental digital content at http://links.lww.com/PAIN/B769). The current densities induced by ATP or by miR-1306-3p were comparable with each other (−103.02 ± 13.59 pA/pF for ATP and −114.53 ± 32.22 pA/pF for miR-1306-3p, respectively, Fig. S3B, available as supplemental digital content at http://links.lww.com/PAIN/B769). When combined, however, ATP (−24.33 ±7.31 pA/pF) and miR-1306-3p (−18.01 ± 4.49)

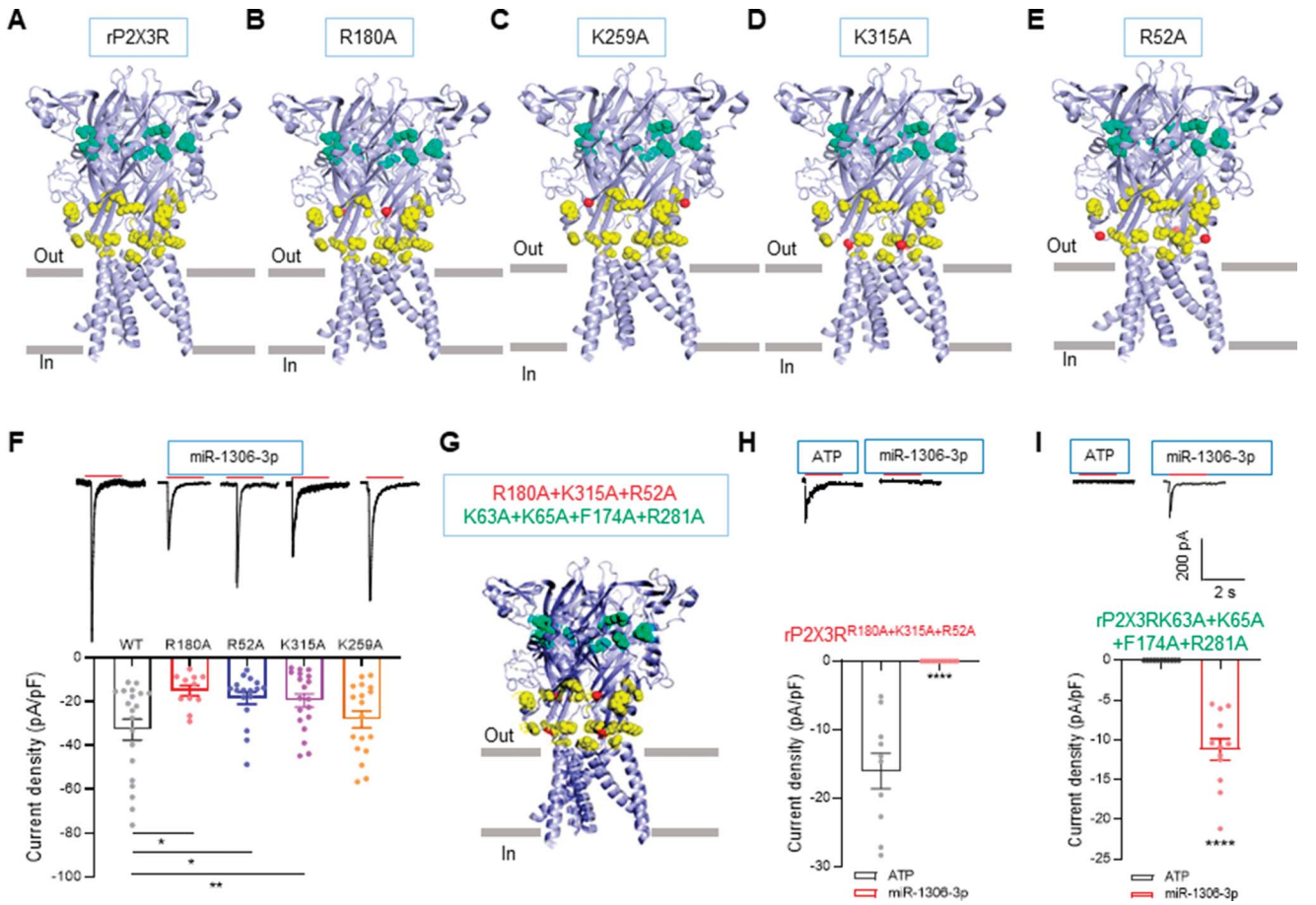

Figure 4. The miR-1306-3p interaction sites (R180, K315, and R52) on P2X3Rs were different from the orthosteric ATP-binding sites. (A-E) The main sites of crystal structure P2X3R bind to miR-1306-3p are R180, K259, K315, and R52, respectively (red balls). (F) The ATP-binding amino acid residues (K63, K65, F174, and R281) and the predicted miR-1306-3p–binding site (R180, K259, K315, and R52) were illustrated as cyan and yellow spheres, respectively. (G) The miR-1306-3p–induced inward currents markedly decreased in the HEK293T cells expressing rP2X3R^{R180A}, rP2X3R^{R52A}, rP2X3R^{K315A}, and rP2X3R^{K259A}. Top: traces of inward currents induced by miR-1306-3p. Bottom: bar graph showing the current density (rP2X3R, n = 25; rP2X3R^{R180A}, n = 13 cells; rP2X3R^{R52A}, n = 20 cells; rP2X3R^{K315A}, n = 22 cells; rP2X3R^{K259A}, n = 20 cells; *$P < 0.05$, one-way ANOVA). (H) Traces and bar graph of ATP-induced inward currents (right) in HEK293T cells expressing rP2X3R$^{R180A+K315A+R52A}$, whereas miR-1306-3p was incapable of inducing currents (ATP, n = 10 cells; miR-1306-3p, n = 11 cells. ****$P < 0.0001$). (I) Traces and bar graph of miR-1306-3p–induced inward currents in HEK293T cells expressing rP2X3R $^{K63A+K65A+F174A+R281A}$, whereas ATP was incapable of inducing currents (ATP, n = 12 cells; miR-1306-3p, n = 12 cells. ****$P < 0.0001$). ANOVA, analysis of variance.

significantly enhanced the current density to −33.55 ± 7.59 pA/pF and −40.72 ± 9.57 pA/pF (**Figs. 5D and E**). Hence, we postulated that at open states (Fig. S3C-F, available as supplemental digital content at http://links.lww.com/PAIN/B769), miR-1306-3p not only altered the overall pore lumen structures (Fig. S3D-F, available as supplemental digital content at http://links.lww.com/PAIN/B769) but also facilitated cations traversing through electrostatic effects of RNA phosphate backbone. We also evaluated the effects of perturbing the miR-1306-3p and P2X3R interactions in animal models. After intrathecal injection of miR-1306-3p antagomir and A317491 together, the CRD thresholds in NCI rats were significantly enhanced (**Fig. 5F**), indicating that miR-1306-3p antagomir and A317491 synergistically attenuated visceral pain.

4. Discussion

Chronic visceral pain is a major threat to global public health.[13] It is often associated with a high comorbidity of stress-related mental diseases, including anxiety and depression, which aggravate the impact on patients and increase the difficulty of pathogenic mechanism research. Therefore, it is of great clinical significance to investigate the mechanisms of visceral pain.[11] This study uncovers a novel mechanism that miR-1306-3p participated in chronic visceral pain. MiR-1306-3p has been previously reported to be involved in tumor cell metastasis and fetal growth restriction research.[44] The downregulation of miR-1306-3p expression was negatively correlated with the pathological characteristics and poor prognosis of gastric cancer.[66] MiR-1306-3p promotes the metastasis of hepatocellular carcinoma in vivo and in vitro by promoting the epithelial–mesenchymal transition process.[17] To our knowledge, there is no report of miR-1306-3p on nervous system diseases nor chronic pain. This study confirmed for the first time that miR-1306-3p directly activates P2X3Rs and excites peripheral primary afferent neurons, thus leading to peripheral sensitization and the development of chronic visceral pain. Our findings not only shed light on the mechanisms underlying chronic visceral pain but also reveal a novel role of miRNA on ion channel functions.

MicroRNA is a small noncoding single-stranded RNA consisting of about 22 nucleotides. They are thought to silence target mRNA by binding to the corresponding 3′-untranslated region (3′-UTR) or open reading frame,[1,22] thus implicated in various physiological and pathological processes, including immune defense, surveillance and homeostasis, tumor promotion, and

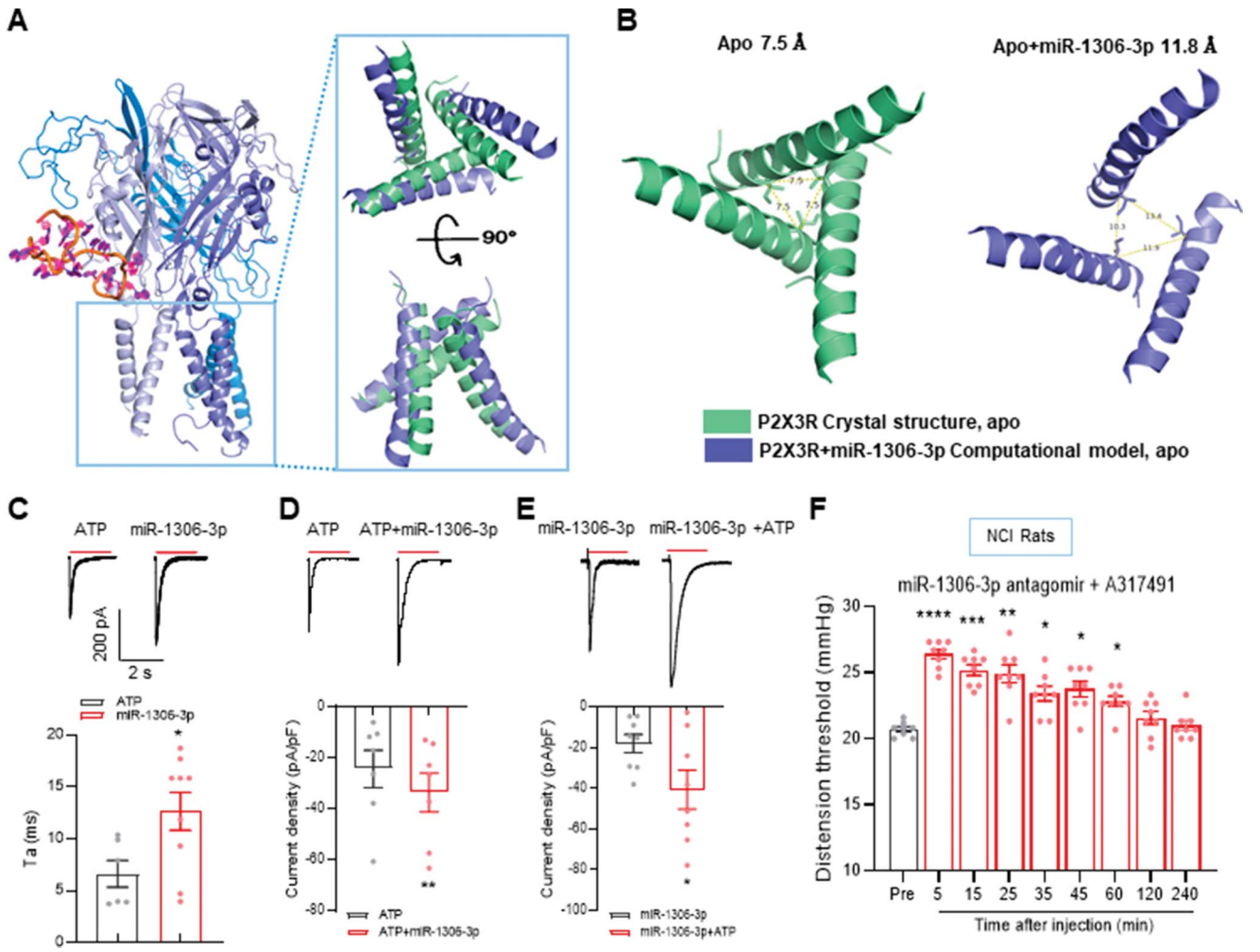

Figure 5. Molecular dynamics equilibrated conformations of the miR-1306-3p–P2X3R complex. (A) Computational models of the miR-1306-3p and P2X3R (apo state) complex. Three protomers of P2X3Rs were illustrated as different shades of blue. MiR-1306-3p binding to the apo P2X3R enlarged the corresponding ion channels, as indicated by comparing the crystal structure (green, without miR-1306-3p) and computational model (blue, with miR-1306-3p binding) at the transmembrane region. (B) The pore size of apo P2X3Rs is 7.5 Å (green), and the pore size of apo P2X3R binding to miR-1306-3p is 11.8 Å (blue). (C) Traces and bar graph statistics showing that inactivation time constant of miR-1306-3p–induced inward current was larger than that of ATP in DRG neurons (ATP, n = 6; miR-1306-3p, n = 9. $^{*}P < 0.05$, *t* test). (D) Traces and bar graph showing that the inward current density of miR-1306-3p and ATP was significantly bigger than that of ATP (n = 7, $^{**}P < 0.01$, *t* test). (E) Traces and bar graph showing that the inward current density induced by miR-1306-3p and ATP was bigger than that of miR-1306-3p in DRG neurons (n = 8 cells, $^{*}P < 0.05$, *t* test). (F) Intrathecal injection of miR-1306-3p antagomir and A317491 (10 μL) significantly enhanced CRD thresholds in NCI rats (n = 6 rats for each group, $^{****}P < 0.0001$, $^{***}P < 0.001$, $^{**}P < 0.01$, and $^{*}P < 0.05$, one-way ANOVA). ANOVA, analysis of variance; CRD, colorectal distension; DRG, dorsal root ganglion.

the regulation of chronic pain.[38,50,55] Recent studies have demonstrated that there are a large number of extracellular miRNAs, which are closely related to expression and function of P2X3Rs.[63] However, whether and how miRNA-1306-3p regulates P2X3R functions remain unknown. This study demonstrates a unique mechanism by which miR-1306-3p participates in the development of chronic visceral pain. Application of miR-1306-3p into acutely dissociated DRG neurons quickly evoked action potentials, increased intracellular calcium mobilization, and induced inward currents. These results strongly indicate that miR-1306-3p plays functions by activating ion channels. By computational stimulations, analysis of inward current characteristics, and surface charges of some ion channels, we suggested that miR-1306-3p most likely activates P2X3Rs. The P2X3R antagonist significantly attenuated the inward currents induced by miR-1306-3p, corroborating the role of miR-1306-3p as P2X3R activators. Although it is difficult to exclude the possibility that some other ion channels or receptors might be associated with the miR-1306-3p functions, we have tried to exclude that TRPV1 or voltage-gated sodium channels in miR-1306-3p mediated effects. Collectively, we demonstrated that miR-1306-3p directly excited DRG neurons by activating P2X3Rs. This conclusion is also supported by a recent study that miR-711 binds to the extracellular fragment of TRPA1 receptors on DRG neurons, activates the TRPA1 channels, and then causes changes in a downstream signal pathway and the regulation of peripheral neurogenesis of itching[15]; also, there are miRNAs that may directly bind intracellular receptors and promote pain or tumor growth.[24,33,62]

In this study, we verify the miR-1306-3p–binding sites on the P2X3Rs. Based on the crystal structures of P2X3Rs,[29] we analyzed the binding mode of miR-1306-3p and P2X3Rs. Four key residues of P2X3Rs that bind to miR-1306-3p, namely, R180, K259, K315, and R52, were identified. Whole-cell patch-clamp recording results indicated that the current recorded from R180, K315, and R52 mutant plasmids was decreased significantly.

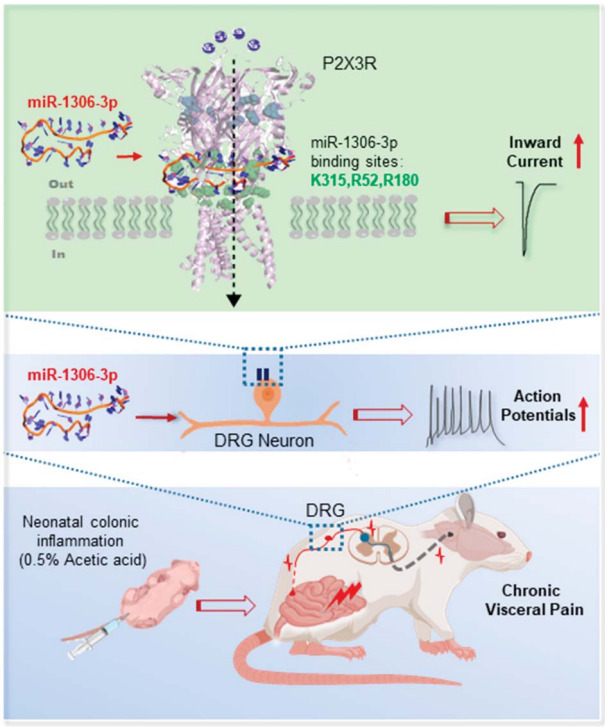

Figure 6. Proposed working model for the role of miR-1306-3p on P2X3R channel dynamics in chronic visceral pain. miR-1306-3p activated P2X3Rs and induced inward current on the DRG neurons, thus increasing the neuron excitability and producing chronic visceral pain. DRG, dorsal root ganglion.

These data strongly suggest that the amino acids of R180, K315, and R52 of P2X3Rs are crucial for miR-1306-3p to bind with.

Because the miR-1306-3p–binding sites are different from ATP, it is therefore interesting to explore how miR-1306-3p binding might affect the ATP effect or the vice versa. The protomer of P2X3Rs contains 2 transmembrane helixes, connected by a large extracellular domain containing ATP-binding sites and N-terminal and C-terminal in different lengths.[21,40,42] A recent study reported the X-ray crystal structure of the P2X3R in the apo/resting state, agonist binding/open state, and agonist binding/desensitization state.[29] Interestingly, our follow-up results showed that P2X3Rs featured an extended period of the open states when miRNA is combined with ATP (Fig. S3E-F, available as supplemental digital content at http://links.lww.com/PAIN/B769). These data represent a novel mechanism that miRNA might act as the "switch" of ion channels, causing the change in the state of ion channels, the ion flow through the cell membrane, and participating in the pathophysiological activities under chronic pain conditions. This conclusion was supported by an observation that a combination of P2X3R antagonist and antagomir of miR-1306-3p had a greater antinociceptive effect than a single use of P2X3R antagonist or antagomir of miR-1306-3p.

A growing body of evidence shows that many miRNAs are contained in and released from the exosomes of the source cells and subsequently absorbed by the target cells.[59] In this study, we showed that miR-1306-3p expression was enhanced in DRG-derived exosomes (**Fig. 1B**). It is, therefore, reasonable to deduce a conclusion that miR-1306-3p was likely released from exosomes and participated in the chronic visceral pain by activating purinergic P2X3Rs. However, the regulatory mechanism by which miR-1306-3p expression was upregulated deserves a further investigation. In addition, further screening of the interaction of miR-1306-3p with other receptors and ion channels and the downstream target molecules of pain information transmission are definitely needed.

In summary, the basic knowledge of the pathogenesis of chronic visceral pain is crucial for the clinical treatment and prevention of the disease. This study focused on the neural mechanism of miR-1306-3p binding to the P2X3Rs on primary sensory afferent neurons. The core sequence of miR-1306-3p binds to the key amino acids on P2X3Rs, which activates the P2X3Rs, induces inward currents, increases the excitability of DRG neurons, and eventually produces visceral pain (**Fig. 6**). We also showed that the application of miR-1306-3p antagomir and A317491 synergistically attenuated visceral pain behaviors of NCI rats, indicating a useful strategy by the combined use of antagonist and antagomir to block the 2 binding sites for ATP and miR-1306-3p. This study not only unveils a novel mechanism underlying the roles of miRNAs but also suggests a novel strategy for the treatment of chronic visceral pain in patients with irritable bowel syndrome.

Conflict of interest statement

The authors have no conflict of interest to declare.

Acknowledgements

This work was supported by grants from the National Natural Science Foundation of China (31730040 and 81920108016 to G.-Y. Xu and 22077094 to C. Zhu) and the Priority Academic Program Development of Jiangsu Higher Education Institutions of China. The calculations were performed on TianHe-1(A).
The funders had no role in the study design, data collection and analysis, decision to publish, or preparation of the manuscript.
Author contributions: Y.-Y. Wu performed experiments, analyzed data, and prepared figures and the manuscript. Q. Wang and P.-A. Zhang analyzed data and revised the manuscript. C. Zhu performed computational simulations and revised the manuscript. G.-Y. Xu designed experiments, supervised the experiments, and finalized the manuscript. All the authors have read and approved the paper.
Ethics approval: Care and handling of the animals were approved by the Institutional Animal Care and Use Committee of Soochow University and were in accordance with the guidelines of the International Association for the Study of Pain.

Appendix A. Supplemental digital content

Supplemental digital content associated with this article can be found online at http://links.lww.com/PAIN/B768 and http://links.lww.com/PAIN/B769.

Supplemental video content

A video abstract associated with this article can be found at http://links.lww.com/PAIN/B770.

Article history:
Received 28 July 2022
Received in revised form 23 October 2022
Accepted 8 November 2022
Available online 22 December 2022

References

[1] Bartel DP. Metazoan MicroRNAs. Cell 2018;173:20–51.

[2] Burnstock G. Physiology and pathophysiology of purinergic neurotransmission. Physiol Rev 2007;87:659–797.
[3] Burnstock G. The therapeutic potential of purinergic signalling. Biochem Pharmacol 2018;151:157–65.
[4] Cha M, Ling J, Xu GY, Gu JG. Shear mechanical force induces an increase of intracellular Ca2+ in cultured Merkel cells prepared from rat vibrissal hair follicles. J Neurophysiol 2011;106:460–9.
[5] Chaplan SR, Bach FW, Pogrel JW, Chung JM, Yaksh TL. Quantitative assessment of tactile allodynia in the rat paw. J Neurosci Methods 1994; 53:55–63.
[6] Chávez J, Vargas MH, Martínez-Zúñiga J, Falfán-Valencia R, Ambrocio-Ortiz E, Carbajal V, Sandoval-Roldán R. Allergic sensitization increases the amount of extracellular ATP hydrolyzed by guinea pig leukocytes. Purinergic Signal 2019;15:69–76.
[7] Chen CC, Akopian AN, Sivilottit L, Colquhoun D, Burnstock G, Wood JN. A P2X purinoceptor expressed by a subset of sensory neurons. Nature 1995;377:428–31.
[8] Chen L, Liu YW, Yue K, Ru Q, Xiong Q, Ma BM, Tian X, Li CY. Differential expression of ATP-gated P2X receptors in DRG between chronic neuropathic pain and visceralgia rat models. Purinergic Signal 2016;12: 79–87.
[9] Chey WD, Kurlander J, Eswaran S. Irritable bowel syndrome: a clinical review. JAMA 2015;313:949–58.
[10] Collo G, North RA, Kawashima E, Merlo-Pich E, Neidhart S, Surprenant A, Buell G. Cloning OF P2X5 and P2X6 receptors and the distribution and properties of an extended family of ATP-gated ion channels. J Neurosci 1996;16:2495–507.
[11] Defrees DN, Bailey J. Irritable bowel syndrome: epidemiology, pathophysiology, diagnosis, and treatment. Prim Care 2017;44:655–71.
[12] Dixon WJ. Efficient analysis of experimental observations. Annu Rev Pharmacol Toxicol 1980;20:441–62.
[13] Gebhart GF, Bielefeldt K. Physiology of visceral pain. Compr Physiol 2016;6:1609–33.
[14] Goudet C, Magnaghi V, Landry M, Nagy F, Gereau RW, Pin JP. Metabotropic receptors for glutamate and GABA in pain. Brain Res Rev 2009;60:43–56.
[15] Han Q, Liu D, Convertino M, Wang Z, Jiang C, Kim YH, Luo X, Zhang X, Nackley A, Dokholyan NV, Ji RR. miRNA-711 binds and activates TRPA1 extracellularly to evoke acute and chronic pruritus. Neuron 2018;99: 449–463. e446.
[16] Hargreaves K, Dubner R, Brown F, Flores C, Joris J. A new and sensitive method for measuring thermal nociception in cutaneous hyperalgesia. PAIN 1988;32:77–88.
[17] He ZJ, Li W, Chen H, Wen J, Gao YF, Liu YJ. miR-1306-3p targets FBXL5 to promote metastasis of hepatocellular carcinoma through suppressing snail degradation. Biochem Biophys Res Commun 2018;504:820–6.
[18] Huang J, MacKerell AD Jr. CHARMM36 all-atom additive protein force field: validation based on comparison to NMR data. J Comput Chem 2013;34:2135–45.
[19] Hultin L, Nissen TD, Kakol-Palm D, Lindström E. Colorectal distension-evoked potentials in awake rats: a novel method for studies of visceral sensitivity. Neurogastroenterol Motil 2012;24:964-e466.
[20] Jelassi B, Anchelin M, Chamouton J, Cayuela ML, Clarysse L, Li J, Goré J, Jiang LH, Roger S. Anthraquinone emodin inhibits human cancer cell invasiveness by antagonizing P2X7 receptors. Carcinogenesis 2013;34: 1487–96.
[21] Jiang LH, Kim M, Spelta V, Bo X, Surprenant A, North RA. Subunit arrangement in P2X receptors. J Neurosci 2003;23:8903–10.
[22] Kabekkodu SP, Shukla V, Varghese VK, D' Souza J, Chakrabarty S, Satyamoorthy K. Clustered miRNAs and their role in biological functions and diseases. Biol Rev 2018;93:1955–86.
[23] Lee JY, Choi HY, Ju BG, Yune TY. Estrogen alleviates neuropathic pain induced after spinal cord injury by inhibiting microglia and astrocyte activation. Biochim Biophys Acta Mol Basis Dis 2018;1864:2472–80.
[24] Lehmann SM, Krüger C, Park B, Derkow K, Rosenberger K, Baumgart J, Trimbuch T, Eom G, Hinz M, Kaul D, Habbel P, Kälin R, Franzoni E, Rybak A, Nguyen D, Veh R, Ninnemann O, Peters O, Nitsch R, Heppner FL, Golenbock D, Schott E, Ploegh HL, Wulczyn FG, Lehnardt S. An unconventional role for miRNA: let-7 activates Toll-like receptor 7 and causes neurodegeneration. Nat Neurosci 2012;15:827–35.
[25] Lewis C, Neidhart S, Holy C, North RA, Buell G, Surprenant A. Coexpression of P2X2 and P2X3 receptor subunits can account for ATP-gated currents in sensory neurons. Nature 1995;377:432–5.
[26] Li H, Wu C, Aramayo R, Sachs MS, Harlow ML. Synaptic vesicles contain small ribonucleic acids (sRNAs) including transfer RNA fragments (trfRNA) and microRNAs (miRNA). Sci Rep 2015;5:14918.
[27] Liu S, Wang M, Wang N, Li S, Sun R, Xing J, Wang Y, Yu S, Li L, Li G, Liang S. Exploring the molecular mechanism of the effect of puerarin on P2X(3). Int J Biol Macromol 2020;142:484–91.
[28] López-Pérez AE, Nurgali K, Abalo R. Painful neurotrophins and their role in visceral pain. Behav Pharmacol 2018;29:120–39.
[29] Mansoor SE, Lü W, Oosterheert W, Shekhar M, Tajkhorshid E, Gouaux E. X-ray structures define human P2X(3) receptor gating cycle and antagonist action. Nature 2016;538:66–71.
[30] Meacham K, Shepherd A, Mohapatra DP, Haroutounian S. Neuropathic pain: central vs. peripheral mechanisms. Curr Pain Headache Rep 2017; 21:28.
[31] Numazaki M, Tominaga M. Nociception and TRP channels. Curr Drug Targets CNS Neurol Disord 2004;3:479–85.
[32] Paredes S, Cantillo S, Candido KD, Knezevic NN. An association of serotonin with pain disorders and its modulation by estrogens. Int J Mol Sci 2019;20:5729.
[33] Park CK, Xu ZZ, Berta T, Han Q, Chen G, Liu XJ, Ji RR. Extracellular microRNAs activate nociceptor neurons to elicit pain via TLR7 and TRPA1. Neuron 2014;82:47–54.
[34] Qi F, Zhou Y, Xiao Y, Tao J, Gu J, Jiang X, Xu GY. Promoter demethylation of cystathionine-beta-synthetase gene contributes to inflammatory pain in rats. PAIN 2013;154:34–45.
[35] Ren Y, Zou X, Fang L, Lin Q. Involvement of peripheral purinoceptors in sympathetic modulation of capsaicin-induced sensitization of primary afferent fibers. J Neurophysiol 2006;96:2207–16.
[36] Rozas G, Labandeira García JL. Drug-free evaluation of rat models of parkinsonism and nigral grafts using a new automated rotarod test. Brain Res 1997;749:188–99.
[37] Sato K, Hamada M, Asai K, Mituyama T. CENTROIDFOLD: a web server for RNA secondary structure prediction. Nucleic Acids Res 2009;37: W277–80.
[38] Sengupta JN, Pochiraju S, Kannampalli P, Bruckert M, Addya S, Yadav P, Miranda A, Shaker R, Banerjee B. MicroRNA-mediated GABA Aα-1 receptor subunit down-regulation in adult spinal cord following neonatal cystitis-induced chronic visceral pain in rats. PAIN 2013;154:59–70.
[39] Sun Q, Zhang BY, Zhang PA, Hu J, Zhang HH, Xu GY. Downregulation of glucose-6-phosphate dehydrogenase contributes to diabetic neuropathic pain through upregulation of toll-like receptor 4 in rats. Mol Pain 2019;15:174480691983865.
[40] Valera S, Hussy N, Evans RJ, Adami N, North RA, Surprenant A, Buell G. A new class of ligand-gated ion channel defined by P2x receptor for extracellular ATP. Nature 1994;371:516–9.
[41] van Aalten DMF, Amadei A, Linssen ABM, Eijsink VGH, Vriend G, Berendsen HJC. The essential dynamics of thermolysin: confirmation of the hinge-bending motion and comparison of simulations in vacuum and water. Proteins 1995;22:45–54.
[42] Vial C, Roberts JA, Evans RJ. Molecular properties of ATP-gated P2X receptor ion channels. Trends Pharmacol Sci 2004;25:487–93.
[43] Vulchanova L, Riedl MS, Shuster SJ, Buell G, Surprenant A, North RA, Elde R. Immunohistochemical study of the P2X2 and P2X3 receptor subunits in rat and monkey sensory neurons and their central terminals. Neuropharmacology 1997;36:1229–42.
[44] Wang G, Yu J, Yang Y, Liu X, Zhao X, Guo X, Duan T, Lu C, Kang J. Whole-transcriptome sequencing uncovers core regulatory modules and gene signatures of human fetal growth restriction. Clin Transl Med 2020; 9:9.
[45] Wang HJ, Xu X, Zhang PA, Li M, Zhou YL, Xu YC, Jiang XH, Xu GY. Epigenetic upregulation of acid-sensing ion channel 1 contributes to gastric hypersensitivity in adult offspring rats with prenatal maternal stress. PAIN 2020;161:989–1004.
[46] Wang J, Xiao Y. Using 3dRNA for RNA 3-D structure prediction and evaluation. Curr Protoc Bioinformatics 2017;57:5.9.1–5.9.12.
[47] Wang S, Zhu HY, Jin Y, Zhou Y, Hu S, Liu T, Jiang X, Xu GY. Adrenergic signaling mediates mechanical hyperalgesia through activation of P2X3 receptors in primary sensory neurons of rats with chronic pancreatitis. Am J Physiol Gastrointest Liver Physiol 2015;308:G710–9.
[48] Wang Z. miRNA in the regulation of ion channel/transporter expression. Compr Physiol 2013;3:599–653.
[49] Wu EL, Cheng X, Jo S, Rui H, Song KC, Dávila-Contreras EM, Qi Y, Lee J, Monje-Galvan V, Venable RM, Klauda JB, Im W. CHARMM-GUI Membrane Builder toward realistic biological membrane simulations. J Comput Chem 2014;35:1997–2004.
[50] Wu R, Zhang PA, Liu X, Zhou Y, Xu M, Jiang X, Yan J, Xu GY. Decreased miR-325-5p contributes to visceral hypersensitivity through post-transcriptional upregulation of CCL2 in rat dorsal root ganglia. Neurosci Bull 2019;35:791–801.

[51] Xu GY, Huang LYM. Peripheral inflammation sensitizes P2X receptor-mediated responses in rat dorsal root ganglion neurons. J Neurosci 2002; 22:93–102.
[52] Xu GY, Huang LYM. Ca2+/calmodulin-dependent protein kinase II potentiates ATP responses by promoting trafficking of P2X receptors. Proc Natl Acad Sci 2004;101:11868–73.
[53] Xu GY, Shenoy M, Winston JH, Mittal S, Pasricha PJ. P2X receptor-mediated visceral hyperalgesia in a rat model of chronic visceral hypersensitivity. Gut 2008;57:1230–7.
[54] Yan Y, Tao H, He J, Huang SY. The HDOCK server for integrated protein-protein docking. Nat Protoc 2020;15:1829–52.
[55] Yi M, Xu L, Jiao Y, Luo S, Li A, Wu K. The role of cancer-derived microRNAs in cancer immune escape. J Hematol Oncol 2020;13:25.
[56] Yuan B, Tang WH, Lu LJ, Zhou Y, Zhu HY, Zhou YL, Zhang HH, Hu CY, Xu GY. TLR4 upregulates CBS expression through NF-κB activation in a rat model of irritable bowel syndrome with chronic visceral hypersensitivity. World J Gastroenterol 2015;21:8615–28.
[57] Zhang F, Ma Z, Weng Z, Zhao M, Zheng H, Wu L, Lu Y, Bao C, Liu Y, Liu H, Wu H. P2X(3) receptor in primary afferent neurons mediates the relief of visceral hypersensitivity by electroacupuncture in an irritable bowel syndrome rat model. Gastroenterol Res Pract 2020;2020:8186106.
[58] Zhang HH, Hu J, Zhou YL, Hu S, Wang YM, Chen W, Xiao Y, Huang LYM, Jiang X, Xu GY. Promoted interaction of nuclear factor-kappaB with demethylated cystathionine-beta-synthetase gene contributes to gastric hypersensitivity in diabetic rats. J Neurosci 2013;33:9028–38.
[59] Zhang J, Li S, Li L, Li M, Guo C, Yao J, Mi S. Exosome and exosomal microRNA: trafficking, sorting, and function. Genomics Proteomics Bioinformatics 2015;13:17–24.
[60] Zhang PA, Zhu HY, Xu QY, Du WJ, Hu S, Xu GY. Sensitization of P2X3 receptors in insular cortex contributes to visceral pain of adult rats with neonatal maternal deprivation. Mol Pain 2018;14: 174480691876473.
[61] Zhang W, Wu H, Xu Q, Chen S, Sun L, Jiao C, Wang L, Fu F, Feng Y, Qian X, Chen X. Estrogen modulation of pain perception with a novel 17β-estradiol pretreatment regime in ovariectomized rats. Biol Sex Differ 2020; 11:2.
[62] Zhang ZJ, Guo JS, Li SS, Wu XB, Cao DL, Jiang BC, Jing PB, Bai XQ, Li CH, Wu ZH, Lu Y, Gao YJ. TLR8 and its endogenous ligand miR-21 contribute to neuropathic pain in murine DRG. J Exp Med 2018;215: 3019–37.
[63] Zhao J, Lee MC, Momin A, Cendan CM, Shepherd ST, Baker MD, Asante C, Bee L, Bethry A, Perkins JR, Nassar MA, Abrahamsen B, Dickenson A, Cobb BS, Merkenschlager M, Wood JN. Small RNAs control sodium channel expression, nociceptor excitability, and pain thresholds. J Neurosci 2010;30:10860–71.
[64] Zhou YL, Jiang GQ, Wei J, Zhang HH, Chen W, Zhu H, Hu S, Jiang X, Xu GY. Enhanced binding capability of nuclear factor-κB with demethylated P2X3 receptor gene contributes to cancer pain in rats. PAIN 2015;156: 1892–905.
[65] Zhu L, Zhao L, Qu R, Zhu HY, Wang Y, Jiang X, Xu GY. Adrenergic stimulation sensitizes TRPV1 through upregulation of cystathionine β-synthetase in a rat model of visceral hypersensitivity. Scientific Rep 2015;5:16109.
[66] Zhu Z, Rong Z, Luo Z, Yu Z, Zhang J, Qiu Z, Huang C. Circular RNA circNHSL1 promotes gastric cancer progression through the miR-1306-3p/SIX1/vimentin axis. Mol Cancer 2019;18:126.